the activation energy are rather small compared to activation energies for HS ⇌ LS transitions in complexes of iron(II).[18,24] A possible explanation may be related to the fact that Fe–ligand bond lengths in nitrosyl iron complexes decrease by about 0.1 Å on conversion from the IS to the LS state,[8] whereas changes about twice as large are encountered for HS ⇌ LS transitions in iron(II) complexes.[14]

Acknowledgment. We thank Dr. S. K. Sengupta for the preparation and magnetic measurements of [Fe(J·mph)NO]. Financial support by the Deutsche Forschungsgemeinschaft, Bonn, Germany, is gratefully acknowledged.

Registry No. [Fe(J·ph)NO], 76683-30-2; [Fe(J·mph)NO], 76683-31-3.

---

(24) König, E.; Ritter, G.; Dengler, J.; Nelson, S. M. *Inorg. Chem.* **1987**, *26*, 3582.

Contribution from Anorganische Chemie III, Eduard-Zintl-Institut
der Technischen Hochschule Darmstadt, D-6100 Darmstadt, Federal Republic of Germany

Kinetic Studies of Nickel(II) and Copper(II) Complexes with N_4 Macrocycles of the Cyclam Type. 1. Kinetics and Mechanism of Complex Formation with Different N-Methylated 1,4,8,11-Tetraazacyclotetradecanes

Jürgen R. Röper and Horst Elias*

Received April 5, 1991

Spectrophotometry and multiscan stopped-flow spectrophotometry was used to study the kinetics of complex formation of divalent transition metal ions M^{2+} (M = Ni, Cu) with the cyclic tetraamines L^1 (=cyclam = 1,4,8,11-tetraazacyclotetradecane), L^2 = (=1-methyl-1,4,8,11-tetraazacyclotetradecane), L^3 (=1,4-dimethyl-1,4,8,11-tetraazacyclotetradecane), L^4 (=1,4,8-trimethyl-1,4,8,11-tetraazacyclotetradecane), and L^5 (=TMC = 1,4,8,11-tetramethyl-1,4,8,11-tetraazacyclotetradecane) in DMF (=*N,N*-dimethylformamide) at an ionic strength of 0.1 M ($NaClO_4$). Complex formation is found to be a two-step process with an initial fast second-order reaction (first-order in both $[M^{2+}]_0$ and $[L]_0$, rate constant k_1), generating an intermediate species $[ML]_{int}{}^{2+}$, and a subsequent slower first-order reaction (rate constant k_2), in which the intermediate is converted to the product $[ML]^{2+}$. At 303 K and for M = Ni second-order rate constant k_1 ranges from 7900 (L^1) to 61 (L^5) $M^{-1}\ s^{-1}$ and follows the relative sequence 130:38:21:9:1 for L^1 to L^5, whereas first-order rate constant k_2 lies in the range 0.1×10^{-3} (L^4) to $0.9 \times 10^{-3}\ s^{-1}$ (L^3), with the exception of $k_2(L^1) = 256 \times 10^{-3}\ s^{-1}$. Even at 218 K the initial step of the reaction of Cu^{2+} ions with L^1–L^4 is too fast to be monitored by the stopped-flow technique. Complex formation of copper(II) with L^5, as studied in the temperature range 215–230 K, is also a two-step process with $k_1 = (8.70 \pm 2.60) \times 10^4\ M^{-1}\ s^{-1}$ (extrapolated value) and $k_2 = (5.40 \pm 0.03) \times 10^{-3}\ s^{-1}$ at 303 K. The activation parameters ΔH^* and ΔS^* for the initial fast reaction in systems Ni^{2+}/L^1–L^5 and Cu^{2+}/L^5 and for the subsequent slow reaction in systems Ni^{2+}/L^5 and Cu^{2+}/L^5 are presented. The visible spectra of the species $[ML]_{int}{}^{2+}$, as obtained by multiscan stopped-flow spectrophotometry, clearly indicate square-planar N_4 coordination of the tetradentate ligands L to the metal in the intermediates. Spectrophotometric titration of $[NiL^5]^{2+}$ and $[CuL^5]^{2+}$ with DMF in nitromethane at 298 K yields the equilibrium constants $K(Ni) = 0.99 \pm 0.05\ M^{-1}$ and $K(Cu) = 30.9 \pm 0.4\ M^{-1}$ for the formation of the monoadducts $[ML^5(DMF)]^{2+}$, respectively. The relative pK_a values of the species LH^+ ($pK_a(1)_r$) and $LH_2{}^{2+}$ ($pK_a(2)_r$) were determined for L^1–L^5 by potentiometric titration in DMF. Increasing N-methylation ($L^1 \rightarrow L^2 \rightarrow L^3 \rightarrow L^4 \rightarrow L^5$) does not affect the size of $pK_a(1)_r$ but reduces the size of $pK_a(2)_r$. A LFE relationship exists between second-order rate constant k_1 and $pK_a(2)_r$, which suggests that formation of the second M–N bond is involved in the rate-controlling step of the formation of $[ML^{2-4}]_{int}{}^{2+}$. ^{1}H-NMR monitoring of the first-order reaction $[NiL^5]_{int}{}^{2+} \rightarrow [NiL^5]^{2+}$ proves that this step corresponds to the isomerization *RSRR*-$[NiL^5]^{2+}$ $\rightarrow$ *RSRS*-$[NiL^5]^{2+}$. It can be concluded from the size of first-order rate constants k_2 that the reactions $[ML^{1-4}]_{int}{}^{2+} \rightarrow [ML^{1-4}]^{2+}$ are also rearrangement reactions, in which a rapidly formed, thermodynamically less stable intermediate isomerizes via M–N bond inversion to form the more stable stereoisomer $[ML]^{2+}$.

Introduction

The fundamental importance and interdisciplinary character of the metal ion chemistry of macrocycles has recently been elegantly described and summarized by Lindoy.[1] Within the huge group of macrocyclic ligands, the aza macrocycles (and, in particular, the tetraaza macrocycles because of their possible relevance to biological systems) have attracted a great deal of attention in the past decades.[2]

A number of investigations of the rates of incorporation of metal ions such as copper(II) and nickel(II) into macrocyclic tetraamines in aqueous solution have appeared.[3] For experimental reasons these studies were carried out in acidic or alkaline media, where either protonation and solvation of the ligand or formation of hydroxo species ($Cu(OH)_3{}^-$ and $Cu(OH)_4{}^{2-}$ in the case of copper) led to problems of interpretation. To avoid these problems, Hay and Norman[4] were the first to use a dipolar aprotic solvent such as acetonitrile for the study of complex formation of nickel(II) with a series of 14-membered macrocyclic and linear N_4 ligands.

---

(1) Lindoy, L. F. *The Chemistry of Macrocyclic Ligand Complexes*; Cambridge University Press: Melbourne, Australia, 1989.

(2) (a) Schwind, R. A.; Gilligan, T. J.; Cussler, E. L. *Synthetic Multidentate Macrocyclic Compounds*; Academic Press: New York, 1978. (b) Melson, G. A. *Coordination Chemistry of Macrocyclic Compounds*; Plenum Press: New York, 1978. (c) Burgess, J. *Metal Ions in Solution*; Ellis Horwood Limited: Chicester, England, 1978.

(3) (a) Margerum, D. W.; Cayley, G. R.; Weatherburn, D. C.; Pagenkopf, G. K. In *Coordination Chemistry*; ACS Monograph 174; American Chemical Society: Washington, DC, 1978; Vol. 2. (b) Kaden, T. A. *Top. Curr. Chem.* **1984**, *121*, 157. (c) Leugger, A.; Hertli, L.; Kaden, T. A. *Helv. Chim. Acta* **1978**, *61*, 2296. (d) Buxtorf, R.; Kaden, T. A. *Helv. Chim. Acta* **1974**, *57*, 1035. (e) Steinmann, W.; Kaden, T. A. *Helv. Chim. Acta* **1975**, *58*, 1358. (f) Schultz-Grunow, P.; Kaden, T. A. *Helv. Chim. Acta* **1978**, *61*, 2291. (g) Hertli, L.; Kaden, T. A. *Helv. Chim. Acta* **1974**, *57*, 1328. (h) Kodama, M.; Kimura, E. *J. Chem. Soc., Dalton Trans.* **1977**, 1473. (i) Drumhiller, J. A.; Montavon, F.; Lehn, J. M.; Taylor, R. W. *Inorg. Chem.* **1986**, *25*, 3751. (j) Chen, F.-T.; Lee, C.-S.; Chung, C.-S. *Polyhedron* **1983**, *2*, 1301.

(4) Hay, R. W.; Norman, P. R. *Inorg. Chim. Acta* **1980**, *45*, L139.

0020-1669/92/1331-1202$03.00/0

Kaden et al.[5] applied the solvents DMSO (=dimethyl sulfoxide) and DMF (=*N,N*-dimethylformamide) for the study of the complexation kinetics of open-chain and cyclic tetraaza ligands with Ni^{2+} ions. The reaction of Cu^{2+} ions with the tetra-N-methylated N_4 macrocycle dibenzocyclam (=TMBC)[6] in DMF was studied by ourselves.[7] Recently Moore et al.[8] investigated the kinetics of complex formation of divalent transition metals with cyclam (=1,4,8,11-tetraazacyclotetradecane), functionalized by the attachment of an additional 2,2′-bipyridyl group, in the solvent DMSO. In addition, one needs to be aware of the kinetic studies carried out on the conversion of thermodynamically less stable configurational isomers of $Ni(TMC)^{2+}$ (TMC = tetra-N-methylated cyclam) to more stable ones in solvents such as DMF and DMSO.[9] It was concluded from such investigations that the solvent is involved in these isomerizations and, for example, the isolation and structural characterization[10] of the five-coordinate species $Ni(TMC)(DMF)^{2+}$ is in line with this interpretation. Furthermore, visible spectroscopy[10-12] and ^1H-NMR measurements[9,13,14] confirmed that in sufficiently polar solvents (S) solvation equilibria involving the species $Ni(TMC)^{2+}$, $Ni(TMC)S^{2+}$, and $Ni(TMC)S_2^{2+}$ play a significant role.

In summarizing the information available on the kinetics of complex formation of transition metal ions M^{2+} with the N_4 macrocycle cyclam and its N-methylated and C-methylated derivatives (L) in dipolar aprotic solvents such as acetonitrile,[4] DMF, and DMSO,[5] one arrives at the following general findings: (i) in most systems studied so far, complex formation is a two-step process, (ii) the initial rapid reaction is first-order in both $[M^{2+}]$ and [L], whereas the subsequent much slower step is independent of $[M^{2+}]$, and (iii) in acetonitrile,[4] N-methylation and C-methylation of cyclam seem to affect the rate of the initial second-order reaction very little, whereas in DMF and DMSO[5] the reaction of nickel(II) with TMC is much slower than with cyclam.

The mechanistic details of complex formation with N_4 macrocycles L of the cyclam type according to the experimentally obtained reaction sequence (1) and (2) (M^{2+} = divalent transition

$$M^{2+} + L \xrightarrow[\text{fast}]{k_1\ (M^{-1}\ s^{-1})} [ML]_{int}^{2+} \qquad (1)$$

$$[ML]_{int}^{2+} \xrightarrow[\text{slow}]{k_2\ (s^{-1})} [ML]^{2+} \qquad (2)$$

metal) are far from well understood. The nature of the intermediate $[ML]_{int}^{2+}$ has not been studied in detail, and consequently, the mechanism of the slow step is still open to discussion. Moreover, the question of whether the first step can be interpreted on the basis of the Eigen–Wilkins mechanism appears to be open.[5] Since coordination of the metal forces the N_4 macrocycle into a highly symmetric arrangement,[15] the question of ligand-controlled (or conformation-controlled) kinetics vs metal-controlled kinetics has not been considered so far.

The present study on the complexation kinetics of nickel(II) and copper(II) with cyclam (L^1)[16] and a series of N-alkylated

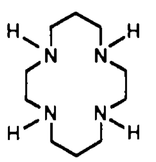
L^1 (cyclam)

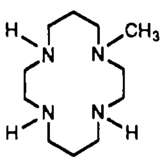
L^2

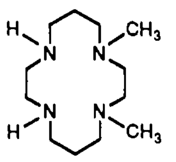
L^3

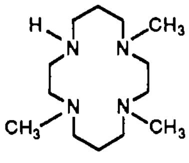
L^4

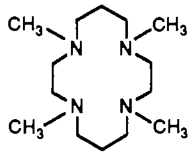
L^5 (TMC)

derivatives of cyclam (L^2–L^5)[16] in DMF according to (3) was

$$M^{2+} + L \rightleftarrows [ML]^{2+} \qquad (3)$$

undertaken to contribute to the understanding of the open mechanistic questions raised above by taking into account the spectroscopic properties of the intermediates $[ML]_{int}^{2+}$ and the relative basicity of the nitrogens in L^1–L^5, as determined from titration studies in DMF.

Experimental Section

Solvents and Reagents. DMF (=*N,N*-dimethylformamide) (Janssen) and nitromethane (Aldrich), both analytical grade, were used without further purification. $[Ni(DMF)_6](ClO_4)_2$ and $[Cu(DMF)_6](ClO_4)_2$ were prepared as described by Fee et al.[17] Tetra-*n*-butylammonium hydroxide (0.1 M solution of $[Bu_4N]OH$ in 2-propanol) and trifluoromethanesulfonic acid (98%) were purchased from Fluka; DMF-d_7 (99.5%) was received from MSD Isotopes.

Caution! Perchlorate salts are explosive and have to be handled carefully.

Ligands. Macrocycles L^1–L^5 were prepared as described in the literature.[18]

Instrumentation: Solution UV/vis absorption spectra, diode array spectrophotometer (HP 8451 A), equipped with a temperature-controlled cell holder; solid-state vis transmission spectra, double-beam spectrophotometer (Zeiss DMR 22), Nujol mull technique; ^1H-NMR spectra, 300-MHz spectrometer (WM 300, Bruker); potentiometric titrations, apparatus (Metrohm) consisting of potentiograph (E 536), titrator (E 538), glass electrode (EA 109), and Ag/AgCl electrode (EA 440; reference) with a salt bridge filled with a saturated solution of LiCl in 2-propanol.

Spectrophotometric Titration. Titration of solutions of $[M(L^5)](ClO_4)_2$ (M = Ni, Cu) in nitromethane with DMF according to (4) was

$$[ML^5]^{2+} + nDMF \rightleftharpoons [ML^5(DMF)_n]^{2+} \quad K \qquad (4)$$

followed spectrophotometrically at 400–800 nm and 298 K. The data obtained for the absorbance *A* at 500 nm (Ni) and 530 nm (Cu), respectively, were computer-fitted to eq 5 (which is valid for the excess

$$K = \{(A - A_0)/(A_\infty - A)\}[DMF]_0^{-n} \qquad (5)$$

condition $[DMF]_0 \gg [ML^5]_0^{2+}$) to determine the parameters *K* and *n*. The symbols A_0 and A_∞ refer to the absorbance of the species $[ML^5]^{2+}$

---

(5) Hertli, L.; Kaden, T. A. *Helv. Chim. Acta* **1981**, *64*, 33.

(6) TMBC = 1,4,8,11-tetramethyl-1,4,8,11-tetraazadibenzo[*b,i*]cyclotetradecane.

(7) Klaehn, D.-D.; Paulus, H.; Grewe, R.; Elias, H. *Inorg. Chem.* **1984**, *23*, 483.

(8) McLaren, F.; Moore, P.; Wynn, A. M. *J. Chem. Soc., Chem. Commun.* **1989**, 798.

(9) (a) Moore, P.; Sachinidis, J.; Willey, G. R. *J. Chem. Soc., Chem. Commun.* **1983**, 522. (b) Lincoln, S. F.; Coates, J. H.; Hadi, D. A. *Inorg. Chim. Acta* **1984**, *81*, L9.

(10) Lincoln, S. F.; Hambley, T. W.; Pisaniello, D. L.; Coates, J. H. *Aust. J. Chem.* **1984**, *37*, 713.

(11) Iwamoto, E.; Yokoyama, T.; Yamasaki, S.; Yabe, T.; Kumamaru, T.; Yamamoto, Y. *J. Chem. Soc., Dalton Trans.* **1988**, 1935.

(12) Crick, I. S.; Tregloan, P. A. *Inorg. Chim. Acta* **1988**, *142*, 291.

(13) Herron, N.; Moore, P. *Inorg. Chim. Acta* **1979**, *36*, 89.

(14) Merbach, A. E.; Moore, P.; Newmann, K. E. *J. Magn. Reson.* **1980**, *41*, 30.

(15) The system Cu^{2+}/TMBC provides a good example for this symmetry argument. As shown by X-ray structure analysis,[7] the molecular structure of the free ligand TMBC[6] lacks any symmetry elements and regularity, whereas in the complex $Cu(TMBC)N_3(ClO_4)$ one finds a highly symmetric arrangement of the macrocycle and the monodentate ligands around the copper.

(16) Abbreviations used: L^1 = cyclam = 1,4,8,11-tetraazacyclotetradecane; L^2 = 1-methyl-1,4,8,11-tetraazacyclotetradecane; L^3 = 1,4-dimethyl-1,4,8,11-tetraazacyclotetradecane; L^4 = 1,4,8-trimethyl-1,4,8,11-tetraazacyclotetradecane; L^5 = TMC = 1,4,8,11-tetramethyl-1,4,8,11-tetraazacyclotetradecane.

(17) Fee, W. W.; McElholum, D. E.; McPherson, A. J.; Rundle, D. L. *Aust. J. Chem.* **1973**, *26*, 1207.

(18) (a) L^1: Barefield, E. K.; Wagner, F.; Herlinger, A. W.; Dahl, A. R. *Inorg. Synth.* **1976**, *16*, 220. (b) L^2: Ciampolini, M.; Fabrizzi, L.; Licchelli, M.; Perotti, A.; Pezzini, F.; Poggi, A. *Inorg. Chem.* **1986**, *25*, 4131. (c) L^3: Barefield, E. K.; Wagner, F.; Hodges, K. D. *Inorg. Chem.* **1976**, *15*, 1370. (d) L^4: Barefield, E. K.; Foster, K. A.; Freeman, G. M.; Hodges, K. D. *Inorg. Chem.* **1986**, *25*, 4663. (e) L^5: Barefield, E. K.; Wagner, F. *Inorg. Chem.* **1973**, *12*, 2435.

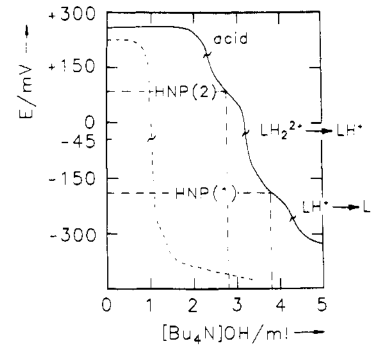

Figure 1. Schematic representation of titration curves obtained in DMF (dashed line, titration of CF_3SO_3H; solid line, titration of quadridentate ligand L in the presence of excess CF_3SO_3H; HNP = half-neutralization potential).

and $[ML^5(DMF)_n]^{2+}$ at initial and final concentration, respectively.

Kinetic Measurements. Complex formation according to (3) was studied in the solvent DMF at $I = 0.1$ M ($NaClO_4$, reagent grade; Janssen) by recording a series of consecutive spectra at adequate time intervals. Reactions with $t_{1/2} > 2$ min were followed by normal spectrophotometry (300–800 nm), whereas faster reactions were monitored with a rapid-scan stopped-flow spectrophotometer[19] (300–725 nm) equipped with a temperature-controlled optical cell (path length = 0.5 cm) allowing measurements down to −90 °C. In the multiscan stopped-flow experiments a total of 90 spectra were taken. In those cases where the initial fast reaction and the subsequent slow reaction were both monitored within one experiment, data sampling was done at two different time bases with 45 spectra being recorded for each reaction. The single spectra were kinetically analyzed at 20 different wavelengths lying within the absorption band of the product. Most of the reactions were studied under stoichiometric conditions ($[M(DMF)_6(ClO_4)_2]_0 = [M]_0 = [L]_0 = 5 \times 10^{-3}$ M) in order to generate spectra of the pure intermediates. The A/t data for the initial fast reaction (A = absorbance; t = time) could be well computer-fitted (least-squares method) to eq 6 (k =

$$A = \{(A_0 - A_\infty)/(1 + k[M]_0 t)\} + A_\infty \qquad (6)$$

second-order rate constant; A_0 and A_∞ refer to $t = 0$ and $t = \infty$, respectively). Some of the experiments were done with a moderate excess of metal salt, i.e. with a ratio $z = [M]_0/[L]_0$ lying in the range 1–10. Under these conditions eq 7 was used to analyze for second-order be-

$$A = \{(A_0 - A_\infty)(z - 1)\exp(-\beta t)\}/\{z - \exp(-\beta t)\} + A_\infty \qquad (7)$$

havior of the initial reaction ($\beta = k[L_0](1 - z^{-1})$). For experiments carried out under pseudo-first-order conditions ($[L]_0 \geq 10[M]_0$ or $[M]_0 \geq 10[L]_0$) and for the separate study of reaction 2, eq 8 was used for

$$A = (A_0 - A_\infty)\exp(-kt) + A_\infty \qquad (8)$$

computer-fitting of the A/t data (k = first-order rate constant). For the investigation of the slow step a total of 30 consecutive spectra were recorded.

NMR Measurements. Solutions (0.3 M) of $[Ni(DMF)_6](ClO_4)_2$ and of the ligand L^5 in DMF-d_7 were mixed at 303 K. The first NMR spectrum was taken immediately after mixing. The reaction of the intermediate $[NiL^5]_{int}^{2+}$ according to (2) was followed by taking another five spectra within 2 h. The NMR signal at 302 ppm indicated the formation of the product $[NiL^5]^{2+}$. To obtain rate constant k_2, the time-dependent integral of this signal was fitted to an exponential with a computer program based on the least-squares method.

Potentiometric Measurements. The ligands L were dissolved in DMF, and a small excess of CF_3SO_3H was added to achieve full protonation of L. These solutions were titrated with a 0.01 M solution of $[Bu_4N]OH$ in 2-propanol at 298 K under nitrogen (see Figure 1). At the end of the titration the solution contained ca. 15 vol % of 2-propanol.

Calculation of Relative pK_a Values. Compared to the medium water, the definition and determination of pK_a values in organic media such as DMF is more complicated and less straightforward. The following procedure provides a *relative* scale of pK_a values of the ligands L^1–L_5 in DMF.

When protonated L is titrated with base in DMF potentiometrically, the continuous change in the potential of the glass electrode (mV) with increasing volume of added base (mL) allows one to determine the half-neutralization potentials (=HNP; see Figure 1). The experimentally

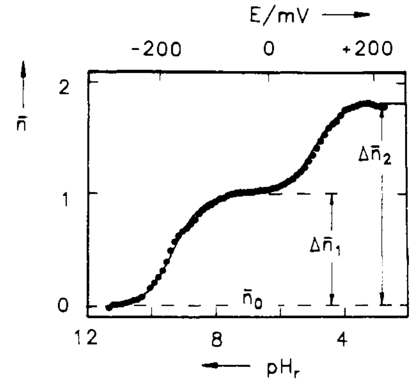

Figure 2. Protonation curve $\bar{n} = f(pH_r)$ of the ligand L^5 in DMF.

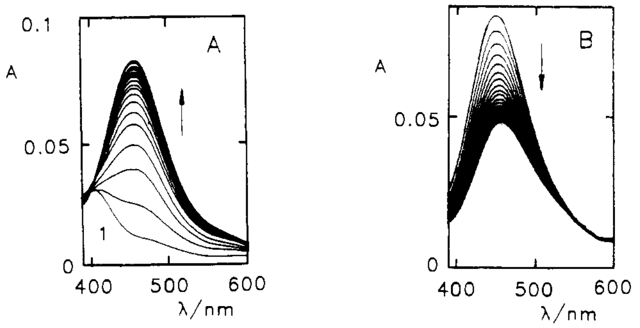

Figure 3. Spectral changes associated with the reaction of Ni^{2+} ions with ligand L^2 ($[Ni^{2+}]_0 = [L^2]_0 = 3.85 \times 10^{-3}$ M) in DMF at 303 K (A, spectrum 1 taken after 10 ms, Δt = time interval between consecutive spectra = 80 ms; B, Δt = 15 min).

obtained mV scale was converted into a relative pH scale on the basis of the following facts, considerations, and assumptions: (i) in water and with the assumption $a(H^+) = [H^+]$, a change in pH by one unit corresponds to a change in the potential of the glass electrode by 59.1 mV (298 K); (ii) repeated titration of CF_3SO_3H with $[Bu_4N]OH$ in DMF yielded a mean potential of −45 mV at the acid:base molar ratio 1:1; (iii) the potential of −45 mV was arbitrarily chosen to represent pH 7 for the system under study, and the relationship 59.1 mV = 1 pH unit was used for scaling.

Equation 9, based on the method suggested by Irving and Rossotti,[20] was used to calculate the parameter $\bar{n}$ (=mean number protons attached

$$\bar{n} = x + [(A_B - A_A) - (A_N + N)(v_B - v_A)(V + v_A)^{-1}]/L_0 \qquad (9)$$

to L) from the titration curves. The symbols in eq 9 have the following meaning: L_0 = initial concentration of L; x = number of acid/base equilibria for L; A_A and A_B = concentration of the anion of the acid upon titration in the absence of L (A) and in the presence of L (B), respectively; N = molarity of the base $[Bu_4N]OH$; V = initial volume of the solution; v_A and v_B = added volume of the solution of the base upon titration in the absence (A) and in the presence of L (B), respectively. As an example, in Figure 2 the data calculated for $\bar{n}$ on the basis of eq 9 are plotted vs the relative pH (pH_r) for the ligand L^5.

For ligands L^1–L^5 only two protonation steps were observed ($x = 2$), according to (10) and (11) (charges omitted):

$$LH_2 \rightleftharpoons LH + H \quad K_2 \qquad (10)$$

$$LH \rightleftharpoons L + H \quad K_1 \qquad (11)$$

Equation 12 describes the function $\bar{n} = f([H])$ on the basis of equilibria (10) and (11):

$$\bar{n} = \frac{\bar{n}_0 + \Delta\bar{n}_1 K^{-1}[H] + \Delta\bar{n}_2 \beta^{-1}[H]^2}{1 + K_1^{-1}[H] + \beta^{-1}[H]^2} \qquad (12)$$

The symbols in this equation have the following meaning (see also Figure 2): $\bar{n}_0$ = limiting value of $\bar{n}$, experimentally obtained after addition of an excess of base; $\Delta\bar{n}_1$ and $\Delta\bar{n}_2$ = change in $\bar{n}$ due to monoprotonation (eq 10) and diprotonation (eq 11) of L, respectively; $\beta = K_1K_2$. The relative pK_a values K_1 and K_2 were obtained by least-squares comput-

---

(19) Wannowius, K. J.; Sattler, F.; Elias, H. *GIT Fachz. Lab.* **1985**, *11*, 1138.

(20) Irving, H. M.; Rosotti, H. S. *J. Chem. Soc.* **1954**, 2904.

Table I. Rate Constants k_1 and k_2 for Complex Formation of Nickel(II) in DMF at 303 K According to Reactions 1 and 2[a]

	ligand				
	L^1	L^2	L^3	L^4	L^5
$10^{-2}k_1$, M^{-1} s^{-1}	79.0 ± 5.3 18 ± 1[b]	23.0 ± 2.5	12.6 ± 1.6 9.85 ± 0.17[c] 6.92 ± 0.17[d]	5.50 ± 0.07	0.610 ± 0.001 0.53 ± 0.01[c] 0.65 ± 0.01[e] 0.75 ± 0.02[f] 0.80 ± 0.03[b] 870 ± 260 (Cu)[g] 72.8 ± 2.1 (Cu)[h]
10^3k_2, s^{-1}	256 ± 7 320 ± 10[b]	0.186 ± 0.001	0.90 ± 0.01 0.70 ± 0.03[c]	0.100 ± 0.003 1.43 ± 0.02 (Cu)[i]	0.580 ± 0.003 0.400 ± 0.003[c] 0.587 ± 0.057[e] 5.40 ± 0.03 (Cu)[i]

[a] Unless stated otherwise, the experiments were carried out under stoichiometric conditions ($[Ni^{2+}]_0 = [L]_0 = 5 \times 10^{-3}$ M). [b] Data referring to 298 K and taken from ref 5. [c] 2-fold excess of nickel(II). [d] 2-fold excess of ligand. [e] Pseudo-first-order conditions with $[Ni^{2+}]_0 \geq 10[L^5]_0$. [f] Pseudo-first-order conditions with $[L^5]_0 \geq 10[Ni^{2+}]_0$. [g] Rate constant k_1 for the reaction of Cu^{2+} with L^5 at 303 K, as calculated from measurements in the temperature range 215–230 K with $\Delta H^* = 15$ kJ mol^{-1} and $\Delta S^* = -101$ kJ mol^{-1} K^{-1}. [h] Rate constant k_1 for the reaction of Cu^{2+} with L^5 at 218 K. [i] Rate constant k_2 for the reaction of Cu^{2+} at 303 K.

er-fitting of the data for $\bar{n}$ and $[H]_{rel}$ to eq 12.

Results and Discussion

General Kinetic Results. The cations $[M(DMF)_6]^{2+}$ absorb at 400 and 670 nm (M = Ni) and at 780 nm (M = Cu), respectively, and do not overlap with the absorption of the species $[NiL]^{2+}$ and $[CuL]^{2+}$ (L = L^1–L^5; for details concerning λ_{max} and ϵ_{max} of the complexes formed, see Table IV). Complex formation can therefore be conveniently followed by monitoring the increase in absorbance in the wavelength range 450–600 nm. One observes biphasic kinetics, as shown in Figure 3 for the system Ni^{2+}/L^2 at 303 K. An initial fast reaction in the millisecond range is followed by a considerably slower reaction in the minute range, which generates the spectrum of $[NiL^2]^{2+}$. Under stoichiometric conditions ($[Ni^{2+}]_0 = [L^2]_0$) and at any wavelength in the range 440–460 nm the change in absorbance associated with the initial reaction follows eq 6, whereas the A/t data for the subsequent slow reaction fit well to eq 8.

This type of kinetic behavior is found for systems Ni^{2+}/L^1–L^5 as well as for the system Cu^{2+}/L^5. Under nonstoichiometric conditions (excess of metal) the A/t data obtained for the initial fast reaction can be well fitted to eq 7 (moderate excess) or eq 8 (large excess), whereas those obtained for the subsequent slow step follow eq 8.

It is thus found that complex formation of Ni^{2+} and Cu^{2+} with ligands L^1–L^5 in DMF is adequately described by second-order reaction 1 (first-order in both M^{2+} and L) and first-order reaction 2 of the intermediate, the rate of which is independent of the concentration of the excess partner M^{2+}. Since the initial reaction is much faster than the consecutive one, both reactions can be studied in isolation.

Kinetic Data for Complex Formation with Nickel(II) and Copper(II). Table I summarizes the rate constants k_1 and k_2 obtained for the reaction of Ni^{2+} ions with ligands L^1–L^5 at 303 K. Increasing N-methylation of cyclam = L^1 has a considerable rate-reducing effect on k_1, which is shown by sequence (13). Rate

$$k_1(L^1):k_1(L^2):k_1(L^3):k_1(L^4):k_1(L^5) = 130:38:21:9:1 \quad (13)$$

constant k_2 is much less affected by increasing N-methylation. With the exception of $k_2(L^1) = 256 \times 10^{-3}$ s^{-1}, rate constants k_2 all lie in the range $(0.1–0.9) \times 10^{-3}$ s^{-1}.

The rate constants reported by Kaden et al.[5] for complex formation in the systems $Ni^{2+}/L^1/DMF$ and $Ni^{2+}/L^5/DMF$ are in more or less acceptable agreement with the present data (see Table I).

The reaction of Cu^{2+} ions with ligands L^1–L^4 is very fast, and the initial fast step could not be traced by the stopped-flow technique even at 218 K.[21] Table I presents therefore rate constant k_1 for the system $Cu^{2+}/L^5/DMF$ only (the values listed were calculated from measurements carried out in the temperature range 215–230 K). The ratio $k_1^{Cu}(L^5)/k_1^{Ni}(L^5)$ amounts to 1.4 × 10^3 at 303 K, which reflects the greater reactivity of Cu^{2+} ions compared with Ni^{2+} ions, well-known from the study of solvent exchange.[22] Interestingly enough, however, rate constant k_2 for the slow step (as presented for systems Cu^{2+}/L^4 and Cu^{2+}/L^5 in Table I) is only by a factor of approximately 10 greater than for the corresponding nickel systems.

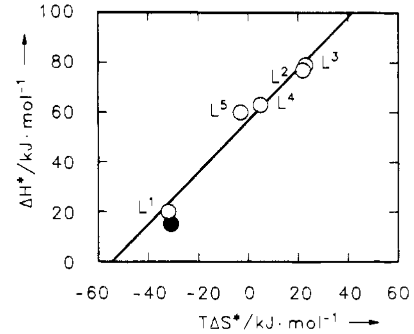

Figure 4. Correleation of the activation parameters ΔH^* and $T(\Delta S^*(303$ K)) for the first step (reaction 1) in system Ni^{2+}/L^1–L^5/DMF. (The symbol ● refers to the system Cu^{2+}/L^5/DMF).

Table II. Activation Parameters for Complex Formation of Nickel(II) in DMF According to Reactions 1[a] and 2[b]

	ligand				
	L^1	L^2	L^3	L^4	L^5
ΔH^*, kJ mol^{-1}	20 ± 2[a]	77 ± 5[a]	79 ± 7[a]	63 ± 2[a]	60 ± 6[a] 67 ± 2[b] 15 ± 6 (Cu)[a] 65 ± 2 (Cu)[b]
ΔS^*, J mol^{-1} K^{-1}	−105 ± 7[a]	74 ± 16[a]	75 ± 23[a]	15 ± 8[a]	−10 ± 18[a] −87 ± 5[b] −101 ± 28 (Cu)[a] −73 ± 8 (Cu)[b]

[a] Data for reaction 1 from the temperature dependence of k_1, as determined at five–eight temperatures in the range 283–313 K. [b] Data for reaction 2 from the temperature dependence of k_2, as determined at five temperatures in the range 231–313 K.

The activation parameters ΔH^* and ΔS^* for intermediate formation in the systems Ni^{2+}/L^1–L^5 according to reaction 1 are summarized in Table II and plotted in Figure 4. The slope of the straight line correlating the parameters ΔH^* and $T\Delta S^*$ is close to 1. This indicates that the formation of the transition state leading to the intermediate is enthalpy-controlled as well as entropy-controlled. For complex formation with the ligand L^5 the activation parameters for both nickel and copper and for both the initial fast step and consecutive slow step are presented. It is

---

(21) DMF solidifies at 212 K, and the kinetic experiments were therefore carried out at $T \geq 218$ K.

(22) Cossy, C.; Helm, L.; Merbach, A. E. *Helv. Chim. Acta* **1987**, *70*, 1516.

Table III. Thermodynamic Parameters for the Solvation Equilibria $[ML^5]^{2+} + n\text{DMF} \rightleftharpoons [ML^5(\text{DMF})_n]^{2+}$ (M = Ni, Cu) As Studied by Spectrophotometric Titration in Nitromethane

M	n^a	K, $M^{-1\,a}$ (298 K)	$\Delta H°$, kJ mol^{-1}	$\Delta S°$, J mol^{-1} K^{-1}	ref
Ni	1	0.99 ± 0.05			this work
		0.80 ± 0.08^b	−16.2 ± 0.5^b	−34.4 ± 1.5^b	this work
		1.2 ± 0.1			11
		0.84	−13.9 ± 1	−26.9 ± 1.5	12
		0.80 ± 0.15	−12.8 ± 2.7	−24.1 ± 9	10
Cu	1	30.9 ± 0.4	−18.9 ± 2.3^c	−34.7 ± 7.2^c	this work

^{a} Obtained by fitting A^{510} (M = Ni) and A^{530} (M = Cu), respectively, to eq 5. ^{b} From the temperature dependence of the visible spectrum of the complex $[NiL^5](ClO_4)_2$ in DMF as recorded at 10 temperatures in the range 294–353 K. ^{c} From titrations at 298, 303, 313, and 323 K.

Table IV. Visible Absorption of Complexes $[NiL]^{2+}_{int}$ and $[NiL]^{2+}$ in DMF (303 K; $c = 5 \times 10^{-3}$ M)

	λ_{max}, nm (ϵ_{max}, M^{-1} cm^{-1})	
	$[NiL]^{2+}_{int}$	$[NiL]^{2+}$
L^1	445 (43)	445 (42)
		523^a
L^2	340 (16), 448 (43)	340 (14), 457 (24)
L^3	467 (54)	471 (65)
		482^b
L^4	375 (12), 472 (40), 605 (sh)	375 (11), 474 (55)
L^5	392 (47), 506 (100), 655 (13)	400 (120), 512 (18), 661 (36)
		514^b
		400 (127), 512 (33), 660 (45)^c
	607 (210)^d	659 (250)^d
		673^e

^{a} Solid-state data for $[CuL^1](ClO_4)_2$. ^{b} Solid-state data for $[NiL^3](ClO_4)_2$. ^{c} From spectrophotometric titration of $[NiL^5]^{2+}$ with DMF in nitromethane at 298 K. ^{d} Data for $[CuL^5]^{2+}_{int}$ and $[CuL^5]^{2+}$, respectively. ^{e} Solid-state data for $[CuL^5(H_2O)](ClO_4)_2$.

important to note that, for the fast step, $\Delta H^{\ddagger}(\text{Ni}) \gg \Delta H^{\ddagger}(\text{Cu})$, whereas for the slow step $\Delta H^{\ddagger}(\text{Ni})$ agrees with $\Delta H^{\ddagger}(\text{Cu})$ within the limits of error.

Solvation of the Species $[NiL^5]^{2+}$ and $[CuL^5]^{2+}$ in DMF. When the visible spectrum of $[NiL^5](ClO_4)_2$ in DMF is taken at different temperatures in the range 20–80 °C, the intensity of the characteristic absorptions at 400 and 661 nm decrease with increasing temperature, whereas the absorption at 512 nm becomes more intense. These changes are due to the temperature dependence of equilibrium (14).[10,12] To determine the parameters K and n,

$$[NiL^5]^{2+} + n\text{DMF} \rightleftharpoons [NiL^5(\text{DMF})_n]^{2+} \quad K \qquad (14)$$

solutions of the complex in nitromethane were titrated spectrophotometrically with DMF and the change in absorbance was fitted to eq 5.[23] With the complex $[CuL^5](ClO_4)_2$ the same type of titration was done at different temperatures.

The results shown in Table III are interesting in the sense that both $[NiL^5]^{2+}$ and $[CuL^5]^{2+}$ add one molecule of DMF ($n = 1$) in an exothermic reaction (see data for ΔH and ΔS) to become five-coordinate. The equilibrium constant K for the formation of the monoadduct is by a factor of 31 higher for the copper complex than for the nickel complex. The value of $K = 0.99$ M^{-1} for the nickel complex means, for example, that the reaction between Ni^{2+} ions and L^5 at 298 K (typically carried out with 5×10^{-3} M solutions) produces a mixture of 7% $[NiL^5]^{2+}$ and 93% $[NiL^5(\text{DMF})]^{2+}$. This formation of DMF adducts is obviously relevant for the discussion of the spectra of the intermediates and products in the kinetic experiments.

It should be pointed out that the present data obtained for K, ΔH, and ΔS in the system $[NiL^5]^{2+}$/DMF are in good agreement with those reported in the literature[10-12] (see Table III).

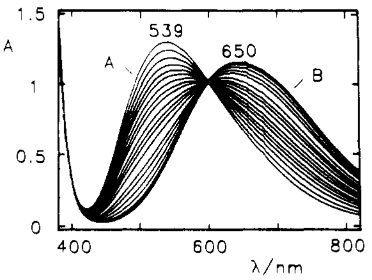

Figure 5. Spectrophotometric titration of $[CuL^5](ClO_4)_2$ (4.83×10^{-3} M; $d = 1$ cm) with DMF in nitromethane at 298 K (A, initial spectrum of $[CuL^5](ClO_4)_2$; B, spectrum at [DMF] = 4.84 M).

Visible Absorption of the Intermediates and Products. Since formation of the intermediate species $[NiL]_{int}^{2+}$ (eq 1) is fast compared to their rearrangement (eq 2), the spectra of the intermediates could be obtained easily (see Table IV). The analysis and comparison of the spectroscopic data obtained for the intermediates and products leads to some interesting findings, namely as follows: (i) the complexes $[NiL^{1-4}]^{2+}$ have a characteristic absorption around 445–474 nm; (ii) the intermediates $[NiL^{1-4}]_{int}^{2+}$ absorb at practically the same wavelengths with absorptivities somewhat smaller (L^2) or greater (L^3, L^4); (ii) as shown for complex $[NiL^3]^{2+}$, absorption in the solid state and in DMF solution occurs at practically the same wavelength; (iv) for DMF solutions of complex $[NiL^5]^{2+}$ the absorption pattern is different in the sense that, in addition to an absorption at 512 nm (514 nm in the solid state), there are two bands at 400 and 661 nm, respectively.

It can be concluded from the known structure of $[NiL^1]Cl_2$[24] that in complexes $[NiL^{1-4}]^{2+}$ the nickel finds itself in the middle of a more or less square-planar N_4 donor atom arrangement. The broad absorption observed in the range 445–474 nm for DMF solutions of complexes $[NiL^{1-4}]^{2+}$ (and also found in the solid state; see $[NiL^3]^{2+}$) is therefore indicative for square-planar N_4 coordination of the nickel.[25] The spectra of the intermediates $[NiL^{1-4}]_{int}^{2+}$ are very close to those of the products $[NiL^{1-4}]^{2+}$, which gives, consequently, strong support to the interpretation that the nickel ion in the intermediates has already arrived at a square-planar N_4 coordination.

For L = L^5 it is again found that both intermediate and product absorb at practically the same wavelength (see Table IV), although with different intensities. The slow step $[NiL^5]_{int}^{2+} \rightarrow [NiL^5]^{2+}$ leads to an increase in absorption at 392 (→400) and 655 (→661) nm and to a decrease at 506 (→512) nm. It is important to note that the kinetically obtained DMF spectrum of $[NiL^5]^{2+}$ is identical with that obtained upon titrating the species $[NiL^5]^{2+}$ with DMF in nitromethane, i.e. with that of five-coordinate $[NiL^5(\text{DMF})]^{2+}$. The kinetically obtained spectrum of the intermediate $[NiL^5]_{int}^{2+}$ with its strong absorption at 506 nm clearly indicates N_4 coordination of the nickel in the intermediate. The reaction $[NiL^5]_{int}^{2+} \rightarrow [NiL^5]^{2+}$ ($t_{1/2}$ = 20 min) is so slow, however, that it cannot represent the addition of DMF to $[NiL^5]^{2+}$, which is known to be an extremely fast process.[10] The intermediate $[NiL^5]_{int}^{2+}$ is therefore a N_4-coordinate species, different though from $[NiL^5]^{2+}$; in the kinetic experiment it is finally converted to $[NiL^5](\text{DMF})^{2+}$.

Discussing the visible absorption of the species $[CuL^5]_{int}^{2+}$ and $[CuL^5]^{2+}$ (see Table IV), one has again to consider the spectral changes associated with the DMF titration of $[CuL^5]^{2+}$ in nitromethane (see Figure 5). Doing so, one arrives at the following

---

(23) Shortly after these titration studies had been carried out Iwamoto et al.[11] published data on the same system.

(24) Bosnich, B.; Mason, R.; Pauling, P. J.; Robertson, G. B.; Tobe, M. L. *J. Chem. Soc., Chem. Commun.* **1965**, 97.

(25) Ligand L^1 = cyclam is known[26] to form the folded macrocyclic complex *cis*-$[NiL^1(H_2O)_2]^{2+}$, which isomerizes slowly[27] in aqueous solution to form the planar complex $[NiL^1]^{2+}$. The spectrum obtained for the intermediate $[NiL^1]_{int}^{2+}$ in the present study (see Table IV) rules out the possibility of $[NiL^1]_{int}^{2+}$ containing the ligand cyclam in the folded geometry.

(26) Billo, E. J. *Inorg. Chem.* **1981**, *20*, 4019.

(27) Billo, E. J. *Inorg. Chem.* **1984**, *23*, 236.

Table V. Half-Neutralization Potentials (HNP), Relative pK_a Values[a] of the Ligands L^1–L^5 in DMF (298 K), and Rate Constants k_1 and k_2 for Reactions 1 and 2 with M = Ni at 298 K

	L^1	L^2	L^3	L^4	L^5
HNP (1), mV	−181 ± 13	−168 ± 0.2	−175 ± 0.3	−187 ± 2.8	−175 ± 5.9
HNP (2), mV	−75 ± 0.2	−21 ± 0.2	+8 ± 1.8	+50 ± 5.9	+73 ± 5.9
$pK_a(1)_r$	9.3 ± 0.2	9.08 ± 0.01	9.20 ± 0.01	9.4 ± 0.1	9.2 ± 0.1
$pK_a(2)_r$	7.5 ± 0.03	6.6 ± 0.02	6.1 ± 0.1	5.4 ± 0.1	5.0 ± 0.1
$pK_a(1)$ (water)	11.83[b]	11.40[c]	10.90[c,d]		10.10[c]
$pK_a(2)$ (water)	10.76[b]	10.35[c]	9.90[c,d]		9.35[c]
$pK_a(3)$ (water)	<2[b]	2.8[c]	3.05[c,d]		3.45[c]
$pK_a(4)$ (water)	<2[b]	~2.3[c]	~2.3[c,d]		~2.7[c]

[a] Calculated on the basis of eq 12. [b] From ref 3c. [c] From ref 3d. [d] Data refer to 1,5-dimethyl-1,5,8,12-tetraazacyclotetradecane (instead of L^3).

conclusions: (i) the strong absorption of the intermediate at 607 nm clearly reflects square-planar N_4 coordination; (ii) the strong absorption at 659 nm observed in the kinetic experiment for the product complex is characteristic for the five-coordinate species $[CuL^5(DMF)]^{2+}$ (for comparison, see Figure 5); (iii) the kinetically observed conversion of the intermediate to the product is a process very different in rate from the addition of DMF to $[CuL^5]^{2+}$.

Relative pK_a Values. Table V summarizes the half-neutralization potentials and relative pK_a values obtained. As pointed out, the deprotonation of only two of the four nitrogens in L is observed upon titration with $[Bu_4N]OH$ in DMF solutions acidified with CF_3SO_3H. The values of $pK_a(1)_r$ characterize the most basic nitrogen N(1) in L. They lie in the narrow range 9.4 (L^4) to 9.08 (L^2). Considering the limits of error, one has to conclude that, in all of the five ligands L^1–L^5, the most basic nitrogen atoms N(1) are practically equally basic. In contrast to $pK_a(1)_r$, the values obtained for $pK_a(2)_r$ decrease continuously from 7.5 (L^1) to 5.0 (L^5). This indicates that stepwise N-methylation of L^1 = cyclam makes the second-basic nitrogen N(2) gradually less basic.

Analyzing the pK_a values reported in the literature for ligands L^1, L^2, and L^5 in water (see Table V), one recognizes the following trends: (i) both $pK_a(1)$ and $pK_a(2)$ decrease with increasing N-methylation; (ii) the difference between $pK_a(1)$ and $pK_a(2)$ is less pronounced than in DMF; (iii) compared to the basicity of nitrogens N(1) and N(2), the basicity of nitrogens N(3) and N(4) is enormously reduced, which is in line with the findings in DMF.

Returning to the relative pK_a values found in DMF, one has to point out that, on the basis of the data presented, an unambiguous stereochemical assignment of the two most basic nitrogens N(1) and N(2) in the N_4 macrocycles L is not possible. This means that N(2) could be located either "cis" or "trans" to N(1). Taking into account, however, that in the cation $[H_2cyclam]^{2+}$ (present in the salt cyclam·$2HClO_4$[28]) the two protonated nitrogens are trans-oriented ones, there is good reason to assume that the second-basic nitrogen N(2) is indeed not neighboring N(1) but located trans to it.

In Figure 6, log k_1 is plotted vs the relative pK_a values of the ligands L^1–L^5. One sees that there is a reasonably linear free energy relationship between log k_1 and $pK_a(2)_r$, the pK_a value characterizing the second-basic nitrogen N(2). This is an interesting finding which proves the rate-affecting role of nitrogen N(2). The less basic N(2) is, the slower the intermediate $[NiL]_{int}^{2+}$ is formed.

It is worthwhile to add that another correlation can be established. As pointed out, the broad absorption observed in the range λ_{max} = 445 (L^1) - 506 (L^5) nm for the intermediates $[NiL^{1-5}]_{int}^{2+}$ (see Table IV) is indicative of square-planar N_4 coordination. When the parameter $(\lambda_{max})^{-1}$ (which is a measure of the transition energy) is plotted versus log k_1, a reasonably linear correlation is again found. This means that decreasing ligand field strength ($L^1 \rightarrow L^5$), which parallels decreasing $pK_a(2)_r$ values, reduces the rate of intermediate formation.

Mechanism of Intermediate Formation According to (1). The discussion of the mechanism of intermediate formation has to consider and take into account the following: (i) the formation of the species $[NiL]_{int}^{2+}$ is a second-order reaction, first-order in both [L] and $[Ni^{2+}]$;[1] (ii) increasing N-methylation of cyclam ($L^1 \rightarrow L^2 \rightarrow L^3 \rightarrow L^4 \rightarrow L^5$) causes a marked decrease in second-order rate constant k_1 (see Table I); (iii) $pK_a(1)_r$, the relative pK_a value of the most basic nitrogen in ligands L^1–L^5, is practically not affected by increasing N-methylation, whereas $pK_a(2)_r$, characterizing the second-basic nitrogen, clearly decreases in the series $L^1 \rightarrow L^5$ (see Table V); (iv) there is a LFE relationship between log k_1 and $pK_a(2)_r$ (see Figure 6); (v) the absorption spectra of the intermediates $[NiL]_{int}^{2+}$ clearly indicate square-planar N_4 coordination of the nickel; (vi) it follows from the activation parameters ΔH^* and ΔS^* that intermediate formation is both enthalpy- and entropy-controlled (see Figure 4); (vii) rate constant k_1 obtained for the systems $Ni^{2+}/L^5/DMF$ and $Ni^{2+}/L^4/DMF$ is considerably smaller than expected on the basis of an Eigen–Wilkins mechanism.

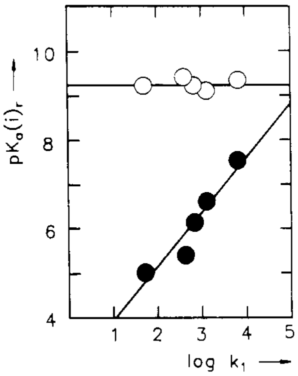

Figure 6. Correlation of rate constant k_1 with $pK_a(1)_r$ (open circles) and $pK_a(2)_r$ (filled circles).

If intermediate formation followed the Eigen–Wilkins mechanism (I_d), formation of the first M–N bond should be rate-determining, which is preceded by outer-sphere complexation (K_{os}) and controlled by the rate of solvent exchange on the metal (k_{ex}). This would imply that $k_1 \approx k_{ex}K_{os}$. Rate constant k_{ex}(DMF) for the Ni^{2+} cation is reported[29] to be 3.8×10^3 s^{-1} at 298 K, which leads to 5.9×10^3 s^{-1} at 303 K. For intermediate formation of Ni^{2+} with the fastest reacting ligand L^1 one finds k_1 = 7900 M^{-1} s^{-1} (see Table I) and, hence, $K_{os} \approx k_1/k_{ex} \approx 1.3$ M^{-1}. This number appears to be of acceptable size for outer-sphere complexation of the type M^{2+}/L(neutral) in an organic solvent such as DMF.[30] So, intermediate formation with L^1 = cyclam could be in line with the mechanistic pattern of the Eigen–Wilkins mechanism. The observed decrease in k_1 (see sequence (13)) from 7900 M^{-1} s^{-1} (L^1) to 61 M^{-1} s^{-1} (L^5), however, remains to be an open question.

Another major argument against the operation of the classical I_d mechanism comes from the finding that all of the intermediates $[NiL]_{int}^{2+}$ are N_4-coordinated already (see Discussion above). Due to stepwise N-methylation, the flexibility of the cyclic ligands L^1–L^5 is increasingly reduced. It is hard to conceive for complex

---

(28) Nave, C.; Truter, M. R. *J. Chem. Soc., Dalton Trans.* **1974**, 2351.

(29) Matwiyoff, N. A. *Inorg. Chem.* **1972**, *11*, 1688.

(30) Wilkins, R. G. *The Study of Kinetics and Mechanism of Reactions of Transition Metal Complexes*; Allyn & Bacon: Boston, MA, 1974; p 183.

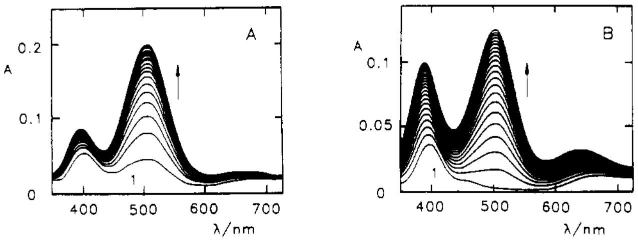

Figure 7. Spectral changes associated with the initial step (reaction 1) in the system $Ni^{2+}/L^5/DMF$ ($[Ni^{2+}]_0 = [L^5]_0 = 4.18 \times 10^{-3}$ M at 303 K (A) and 243 K (B); spectrum 1 taken after 10 ms; A, Δt = time interval between consecutive spectra = 0.4 s; B, Δt = 10 s)).

Scheme I. Mechanism of Intermediate Formation (Charges Omitted; M = Ni, S = Solvent)

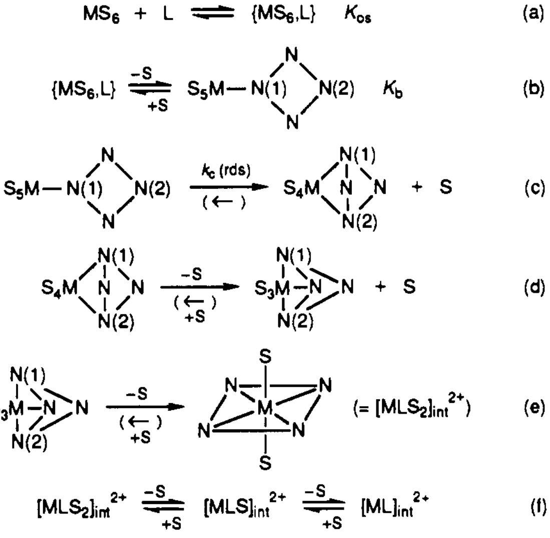

formation with these ligands that the series of ring closure steps following the formation of the first M–N bond should be fast consecutive reactions. The reaction of Ni^{2+} with L^5 = TMC was additionally investigated at low temperatures (243 instead of 303 K). Figure 7 shows that, due to the temperature dependence of intermediate solvation, the intensity of the "square-planar band" at 505 nm has decreased. Except for this change in relative band intensities, however, there is no evidence for the formation of any new, spectroscopically different species. So, even at −30 °C, the stopped-flow experiment generates spectra clearly indicative of N_4 coordination. In addition, there are no biphasic kinetics to be observed at the low temperature of 243 K are rate constant k_1 obtained at 243 K agrees well with the one obtained by extrapolation of k_1(303 K) to 243 K.

Scheme I presents a mechanism which takes into account the sum of the experimental findings. After rapid outer-sphere complexation according to equilibrium (a), the first M–N bond is formed in step (b). It is very reasonable to postulate that it is the most basic nitrogen N(1) to form this bond. At least for ligands L^2–L^5, formation of the M–N(1) bond is obviously no longer rate-determining. Increasing N-methylation of L makes step (c) rate-controlling instead. Since N(2) is probably located "trans" to N(1) (see Discussion above), the quadridentate ligand L has to adopt a folded, butterfly-like conformation in the species $[S_4ML]^{2+}$ formed in step (c). Model considerations indicate that, for such a coordination, the ligand L obviously can more easily occupy two trans-located coordination sites of the metal than two cis-located ones. Further loss of a solvent molecule according to step (d) then leads to a probably meridional N_3 coordination[31] of L in the species $[S_3ML]^{2+}$. In step (e) this species is finally converted to the intermediate $[ML]_{int}^{2+}$ with L being N_4-coordinated in a square-planar arrangement. Depending on the nature of L, the intermediate can be more or less solvated, so that, according to equilibria (f), the species $[MLS]_{int}^{2+}$ and $[MLS_2]_{int}^{2+}$ have to be taken into account in addition.

Scheme I considers steps (a) and (b) (at least for ligands L^2–L^5) to be fast equilibria. The rate-controlling closure of the first chelate ring according to step (c) is followed by steps (d) and (e) as fast and quasi-irreversible consecutive reactions. Since the kinetic data obtained upon studying reaction 1 under stoichiometric conditions ($[M]_0 = [L]_0$) did not provide any evidence for reversibility, step (c) has also to be considered as being quasi-irreversible. It follows, therefore, that the experimental rate constant k_1 should correspond to the product $K_{os}K_bk_c$. This means that the activation parameters derived from the temperature dependence of k_1 are of limited mechanistic value only. Assuming that equilibrium constant K_{os} for ligands L^1–L^5 is practically of the same size, one is left with the question of whether K_b or k_c controls the observed decrease in k_1 with increasing N-methylation. It is undoubtedly reasonable to argue that the size of K_b should follow the basicity of nitrogen N(1), which is constant, however, and not affected by N-methylation. So, the most straightforward interpretation appears to be the postulate that rate constant k_c is responsible for the observed changes in the rate of intermediate formation. The correlation shown in Figure 6 proves that the basicity of the second-basic nitrogen N(2) is at least one of the factors controlling the size of k_c. Another factor could well be the conformational flexibility of the ligand L, which is affected by N-methylation of L. The rate of step (c) will correspond to the rate at which the N(1)-bound ligand L can bring its nitrogen N(2) into the right position relative to a vacant site on the metal. The latter rate is controlled by the rate of conformational change in L.

In summary, only the rate of formation of the intermediate $[Ni(cyclam)]_{int}^{2+}$ is convincingly compatible with the rate of DMF exchange on the nickel. Formation of the species $[NiL^{2-4}]_{int}^{2+}$ is increasingly slower than expected for solvent exchange control. Scheme I presents a mechanism which can account for the observed decrease in k_1 with increasing N-methylation of cyclam. It postulates that, for ligands L^2–L^5, there is no longer "metal control" according to step (b) but "ligand control" according to step (c).

Assuming that Scheme I holds for M = Ni as well as for M = Cu, the ratio $k_1(Cu){:}k_1(Ni)$ for a given ligand L should shed some light on the question of metal-controlled kinetics vs ligand-controlled kinetics. The study of intermediate formation in the systems Ni^{2+}/L^5 (studied at 303 K) and Cu^{2+}/L^5 (studied at 218 K) leads (by extrapolation of the copper data to 303 K) to the ratio $k_1(Cu){:}k_1(Ni) = 1.7 \times 10^3$. The rate constants available for methanol exchange in solvated Cu^{2+} ions and Ni^{2+} ions, respectively, differ by a factor of ca. 3.1×10^4 at 298 K.[32] Assuming that this factor is valid for the solvent DMF as well, one could argue that the experimentally obtained factor of only 1.7×10^3 is indeed an indication for the rate of conformational change in L^5 becoming rate-affecting.

Mechanism of Intermediate Rearrangement According to (2). The mechanistic discussion of this comparatively slow consecutive reaction has to accommodate the following facts: (i) the reaction is first-order in $[NiL]_{int}^{2+}$ and the corresponding rate constant k_2 is fairly constant for ligands L^2–L^5 $(0.1–0.9) \times 10^{-3}$ s^{-1} (see Table I) with the exception of $L = L^1$ (256×10^{-3} s^{-1}); (ii) the absorption spectra of $[NiL]_{int}^{2+}$ indicate planar N_4 coordination and are very close to those of the products $[NiL]^{2+}$; (iii) the copper intermediates $[CuL^4]_{int}^{2+}$ and $[CuL^5]_{int}^{2+}$ react only 10 times faster than the analogous nickel intermediates (see Table I) and the corresponding activation parameters agree within error (see Table II).

A reasonable interpretation of these findings comes from the earlier suggested assumption[4-7] that reaction 2 is a reorganization

---

[31] Meridional N_3 coordination was also found for the complex $[Mo(CO)_3L]$, formed in the reaction of $[Mo(CO)_6]$ with the tetraaza macrocycle Tet A (Hay, R. W.; Fraser, I.; Ferguson, G. *J. Chem. Soc., Dalton Trans.* **1989**, 2183).

[32] Helm, L.; Lincoln, S. F.; Merbach, A. E.; Zbinden, D. *Inorg. Chem.* **1986**, *25*, 2550.

Table VI. Rate Constants for the First-Order Reaction $[NiL^5]^{2+}_{int} \rightarrow [NiL^5]^{2+}$ in DMF

reacn studied	exptl method	k, s^{-1}	T, K	ref
$[NiL^5]^{2+}_{int} \rightarrow [NiL^5]^{2+}$	vis spectroscopy	$5.8 \times 10^{-4} \pm 2.5 \times 10^{-6}$	303	this work
$[NiL^5]^{2+}_{int} \rightarrow [NiL^5]^{2+}$	^1H-NMR (302 ppm signal)	$5.2 \times 10^{-4} \pm 9.1 \times 10^{-5}$	303	this work
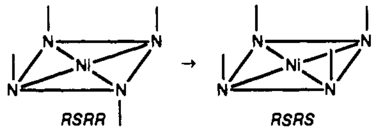	^{13}C-NMR	$\sim 4.6 \times 10^{-4}$	298.2	9b
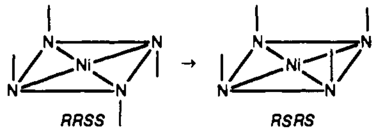	^1H-NMR	$\sim 1 \times 10^{-4}$	362	9a

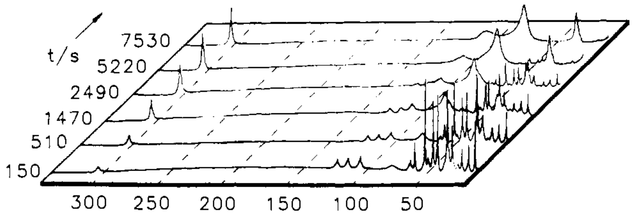

Figure 8. Time dependence of ^1H-NMR spectra describing the reaction $[NiL^5]_{int}^{2+} \rightarrow [NiL^5]^{2+}$ at 303 K in DMF-d_7 in the range $\delta = 10$–340 ppm.

step in which the intermediate $[ML]_{int}^{2+}$, rapidly formed in step (1) with planar N_4M coordination geometry, is converted to a thermodynamically more stable stereoisomer $[ML]^{2+}$ as product. Support for this interpretation follows from ^1H-NMR monitoring of the reaction $[Ni(TMC)]_{int}^{2+} \rightarrow [Ni(TMC)]^{2+}$ in DMF-d_7 at 303 K in the range $\delta = 10$–340 ppm (see Figure 8). First of all, one recognizes a strong and constant paramagnetic shift of the signals of the ligand TMC throughout the rearrangement step and also line broadening. This means that there is not formation of a diamagnetic intermediate but formation of a paramagnetic solvated species $[Ni(TMC)S_x]_{int}^{2+}$ ($x = 1, 2$) instead. Second, the final spectrum is identical with that of $[Ni(TMC)](ClO_4)_2$ in DMF-d_7 and with that of $[Ni(TMC)Cl]^+$, in which the ligand is coordinated in the trans I (*RSRS*) configuration.[13] The final spectrum disagrees with that of the trans II (*RRSS*) isomer of $[Ni(TMC)]^{2+}$.[9a,14] This is in line with the interpretation that the final product in the kinetic experiment is the trans I (*RSRS*) configurated species $[Ni(TMC)(DMF)]^{2+}$, with the four methyl groups and one coordinated DMF molecule located on one side of the N_4Ni coordination plane.[10]

The time dependence of the NMR spectra shown in Figure 8 demonstrates the transition from a multiline spectrum to a four-line spectrum. The detailed analysis of the initial fine structure of the spectrum, as based on the NMR data reported[13] for the various stereoisomers of $[Ni(TMC)]^{2+}$, leads to the conclusion that the first-order reaction of the intermediate $[Ni(TMC)]_{int}^{2+}$ corresponds to isomerization (15). The rate of reaction 15 is thus obviously controlled by Ni–N bond inversion. The time dependence of the NMR signals (see Figure 8) yields the first-order rate constant $k = 5.2 \times 10^{-4}$ s^{-1}, which is in acceptable agreement with the spectrophotometrically determined rate constant $k = 5.8 \times 10^{-4}$ s^{-1} (see Table VI). Moreover, an earlier ^{13}C-NMR study[9b] of the isomerization reaction *RSRR*-$[Ni(TMC)]^{2+} \rightarrow$ *RSRS*-$[Ni(TMC)]^{2+}$ led to $k = 4.6 \times 10^{-4}$ s^{-1} at 298 K, which supports the interpretation given in (15). The isomerization of the *RRSS*-isomer, which also yields the *RSRS*-isomer, was found to be much slower[9a] (see Table VI).

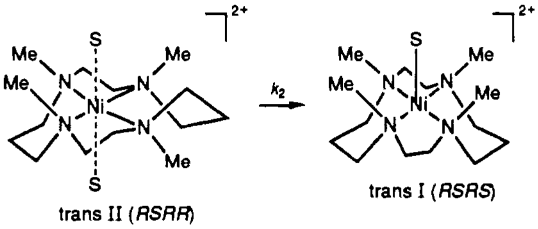

(15)

The data for rate constant k_2 of the slow reaction of the intermediate $[NiL^{2-5}]_{int}^{2+}$ are very similar (mean 0.44×10^{-3} s^{-1}; see Table I). If, as described in reaction 15, the k_2 step of the intermediate $[NiL^5]_{int}^{2+}$ is an isomerization reaction involving N-inversion, it is reasonable to postulate that the intermediates $[NiL^{2-4}]_{int}^{2+}$, all reacting at practically the same rate, are thermodynamically unstable isomers as well. In contrast to the stereochemically well-characterized reaction 15 the configurational changes associated with the isomerizations $[NiL^{1-4}]_{int}^{2+} \rightarrow [NiL^{1-4}]^{2+}$ are not known so far. As a matter of fact, even the products $[NiL^{2-4}]^{2+}$ are stereochemically not characterized. It is reasonable to assume, however, that, similar to $[NiL^1]Cl_2$,[24] the cations $[NiL^{2-4}]^{2+}$ are of the *RRSS*-type. If so, the present data allow not more than the statement that the configuration of the intermediates $[NiL^{1-4}]_{int}^{2+}$ is not of the *RRSS*-type.

The general conclusion is, therefore, that in the course of the rather fast process of intermediate formation there is not enough time for the cyclic ligand to accommodate the metal in the thermodynamically most stable configuration. The latter is formed in a subsequent first-order step, which is slow, because of N-inversion(s) being involved. The number of *N*-methyl groups present in L^2–L^5 is not systematically reflected by the size of k_2. This could mean that the introduction of just one *N*-methyl group is enough to make any Ni–N bond inversion in the intermediate energetically more difficult. The ratio $k_2(L^1):k_2(L^{2-5}) \approx 600$ is surprisingly high though and difficult to understand as well as the ratio $k_2(Cu):k_2(Ni) \approx 10$, as obtained for L^4 and L^5 (see Table I). In general, copper(II) complexes are thermodynamically more stable than nickel(II) complexes and one could expect, therefore, that inversion processes in $[CuL]_{int}^{2+}$ are slower than in $[NiL]_{int}^{2+}$.

Billo[26,27] found that cyclam can form the folded macrocyclic complex *cis*-$[NiL^1(H_2O)_2]^{2+}$, which isomerizes slowly in aqueous solution to form the planar species $[NiL^1]^{2+}$. The corresponding spectra rule out that the intermediate species $[NiL^1]_{int}^{2+}$, as observed in the present kinetic study, is an isomer with the ligand cyclam in the folded geometry. Moreover, it was shown that *cis*-$[NiL^1(H_2O)_2](ClO_4)_2$, dissolved in DMF, is stable for weeks and does not isomerize.

Conclusions

As described by eqs 1 and 2, complex formation of divalent transition metal ions with cyclam and its N-methylated derivatives in DMF is a two-step process. The intermediate $[ML]_{int}^{2+}$, formed in the first step, has already achieved square-planar N_4M coordination. It is thermodynamically unstable and converted to the product $[ML]^{2+}$ in a comparatively slow consecutive reaction (second step). The relative pK_a of the second-basic nitrogens in ligands L, as determined by titration in DMF, correlates with the second-order rate constants k_1 for the first step. This correlation suggests that, along with increasing N-methylation of cyclam, the rate of intermediate formation is controlled by the rate of formation of the second M–N bond. It follows from ^1H-NMR studies that the second step is a rearrangment reaction of the intermediate involving M–N bond inversion. The complex $[ML]^{2+}$, finally formed, is a thermodynamically more stable stereoisomer of the intermediate $[ML]_{int}^{2+}$.

Acknowledgment. Sponsorship of this work by the Deutsche Forschungsgemeinschaft and by the Verband der Chemischen Industrie e.V. is gratefully acknowledged.

Registry No. L^1, 295-37-4; L^2, 53118-99-3; L^3, 121187-41-5; L^4, 67707-85-1; L^5, 41203-22-9; Ni, 7440-02-0; Cu, 7440-50-8.

Contribution from Anorganische Chemie III, Eduard-Zintl-Institut
der Technischen Hochschule Darmstadt, D-6100 Darmstadt, Federal Republic of Germany

Kinetic Studies of Nickel(II) and Copper(II) Complexes with N_4 Macrocycles of the Cyclam Type. 2. Kinetics and Mechanism of Complex Formation with Different C-Alkylated 1,4,8,11-Tetraazacyclotetradecanes

Jürgen R. Röper and Horst Elias*

Received April 5, 1991

The relative pK_a values of the species LH^+ (p$K_a(1)_r$) and LH_2^{2+} (p$K_a(2)_r$) were determined for six cyclic tetraamines L^6 (=-1,4,8,11-tetraazadibenzo[*b,i*]cyclotetradecane), L^7 (=TMBC = 1,4,8,11-tetramethyl-1,4,8,11-tetraazadibenzo[*b,i*]cyclotetradecane), L^8 (=Tet A = *meso*-5,5,7,12,12,14-hexamethyl-1,4,8,11-tetraazacyclotetradecane), L^9 (=Tet B = *rac*-5,5,7,12,12,14-hexamethyl-1,4,8,11-tetraazacyclotetradecane), L^{10} (=*meso*-5,12-dimethyl-1,4,8,11-tetraazacyclotetradecane), and L^{11} (=*meso*-5,12-dimethyl-*meso*-7,14-diphenyl-1,4,8,11-tetraazacyclotetradecane) by potentiometric titration in *N,N*-dimethylformamide (=DMF). p$K_a(1)_r$ and p$K_a(2)_r$ are not significantly affected by C-alkylation within the series of ligands L^6–L^{11}. Spectrophotometry and multiscan stopped-flow spectrophotometry was used to study the kinetics of complex formation of M^{2+} ions (M = Ni, Cu) with L^6–L^{11} in DMF at $I = 0.1$ M ($NaClO_4$) in the temperature ranges 293–313 K (Ni) and 215–263 K (Cu), respectively. Complex formation is found to be a two-step process with an initial fast second-order reaction (first-order in both $[M^{2+}]_0$ and $[L]_0$, rate constant k_1), generating an intermediate species $[ML]_{int}^{2+}$, and a subsequent slower first-order reaction (rate constant k_2), in which the intermediate is converted to the product $[ML]^{2+}$. The activation parameters ΔH^* and ΔS^* of the k_1 step are reported for systems M^{2+}/L^{6-11}. At 303 K and for M = Ni, rate constant k_1 ranges from 1040 (L^{10}) to 0.057 $M^{-1}\,s^{-1}$ (L^7), whereas rate constant k_2 lies in the range 1.5×10^{-3} (L^{11}) to $0.08 \times 10^{-3}\,s^{-1}$ (L^9). For M = Cu, k_1(218 K) ranges from 14.4×10^4 (L^9) to 0.0283 $M^{-1}\,s^{-1}$ (L^7), and k_2(303 K) ranges from 83.7×10^{-3} (L^7) to $0.54 \times 10^{-3}\,s^{-1}$ (L^{10}). The characteristics of the visible absorption spectra of the intermediates $[ML]_{int}^{2+}$ and products $[ML]^{2+}$ are presented. They clearly indicate square-planar N_4 coordination of L in the intermediates as well as in the products. Only the nickel species formed with L^6 and L^7 are different in that the ligand is probably folded. The kinetic data obtained are not in line with the interpretation that intermediate formation follows the classical Eigen–Wilkins mechanism with the formation of the first M–N bond being rate-controlling. They suggest instead the operation of a mechanism with conformational changes in the ligands affecting rate control (Eigen–Winkler mechanism).

Introduction

As shown in the preceding contribution,[1] complex formation of divalent transition metal ions M^{2+} (M = Ni, Cu) with the tetraaza macrocycle cyclam (=L^1)[2] and differently N-methylated cyclam ligands (L^2–L^5)[2] in the aprotic solvent DMF (=*N,N*-dimethylformamide) is a two-step process according to (1) and (2).

$$M^{2+} + L \xrightarrow{k_1\,(M^{-1}\,s^{-1})} [ML]_{int}^{2+} \qquad (1)$$

$$[ML]_{int}^{2+} \xrightarrow{k_2\,(s^{-1})} [ML]^{2+} \qquad (2)$$

The visible spectra of the intermediates $[ML]_{int}^{2+}$, formed according to (1), clearly indicate square-planar N_4 coordination.[1] Second-order rate constant k_1 correlates with the pK_a of the second-basic nitrogen of ligands L^1–L^5, which suggests the formation of the second M–N bond to be the rate-controlling step in the formation of $[ML]_{int}^{2+}$.[1] There is strong experimental evidence in support of reaction 2 being an isomerization step, in which the thermodynamically less stable intermediate forms the more stable stereoisomer $[ML]^{2+}$ via M–N bond inversion.[1]

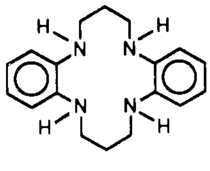

L^6

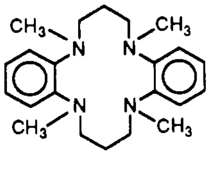

L^7 (TMBC)

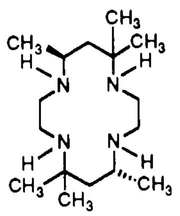

L^8 (TET A)

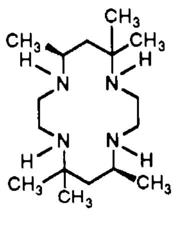

L^9 (TET B)

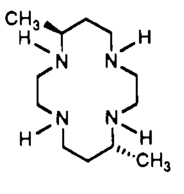

L^{10}

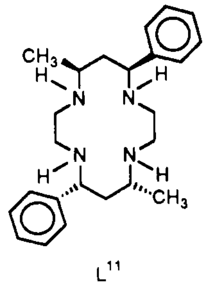

L^{11}

In the present contribution the kinetic investigation of complex formation with N-methylated cyclam derivatives L^2–L^5 is extended to C-alkylated cyclam derivatives L^6–L^{11}.[3] The study was undertaken (i) to provide data for a comparison of the kinetic effect of C-alkylation vs N-alkylation and (ii) to address the question of ligand-controlled kinetics vs metal-controlled kinetics on the basis of the data obtained for nickel(II) and copper(II) reacting

---

(1) Röper, J. R.; Elias, H. *Inorg. Chem.*, preceding paper in this issue.

(2) Abbreviations used: L^1 = cyclam = 1,4,8,11-tetraazacyclotetradecane; L^2 = 1-methyl-1,4,8,11-tetraazacyclotetradecane; L^3 = 1,4-dimethyl-1,4,8,11-tetraazacyclotetradecane; L^4 = 1,4,8-trimethyl-1,4,8,11-tetraazacyclotetradecane; L^5 = TMC = 1,4,8,11-tetramethyl-1,4,8,11-tetraazacyclotetradecane.

(3) Abbreviations used: L^6 = 1,4,8,11-tetraazadibenzo[*b,i*]cyclotetradecane; L^7 = TMBC = 1,4,8,11-tetramethyl-1,4,8,11-tetraazadibenzo[*b,i*]-cyclotetradecane; L^8 = Tet A = *meso*-5,5,7,12,12,14-hexamethyl-1,4,8,11-tetraazacyclotetradecane; L^9 = Tet B = *rac*-5,5,7,12,12,14-hexamethyl-1,4,8,11-tetraazacyclotetradecane; L^{10} = *meso*-5,12-dimethyl-1,4,8,11-tetraazacyclotetradecane; L^{11} = *meso*-5,12-dimethyl-*meso*-7,14-diphenyl-1,4,8,11-tetraazacyclotetradecane.

0020-1669/92/1331-1210$03.00/0 © 1992 American Chemical Society